Using miniature sensor coils for simultaneous measurement of orientation and position of small, fast-moving animals

Schilstra, C.; Hateren, J.H. van

Published in:
Journal of Neuroscience Methods

Publication date:
1998

ELSEVIER

Journal of Neuroscience Methods 83 (1998) 125–131

JOURNAL OF NEUROSCIENCE METHODS

Using miniature sensor coils for simultaneous measurement of orientation and position of small, fast-moving animals

C. Schilstra, J.H. van Hateren *

Department of Neurobiophysics, University of Groningen, Nijenborgh 4, Groningen, NL-9747 AG, The Netherlands

Received 19 January 1998; accepted 9 March 1998

Abstract

A system is described that measures, with a sampling frequency of 1 kHz, the orientation and position of a blowfly (*Calliphora vicina*) flying in a volume of $0.4 \times 0.4 \times 0.4$ m^3. Orientation is measured with a typical accuracy of 0.5°, and position with a typical accuracy of 1 mm. This is accomplished by producing a time-varying magnetic field with three orthogonal pairs of field coils, driven sinusoidally at frequencies of 50, 68, and 86 kHz, respectively. Each pair induces a voltage at the corresponding frequency in each of three miniature orthogonal sensor coils mounted on the animal. The sensor coils are connected via thin (12-μm) wires to a set of nine lock-in amplifiers, each locking to one of the three field frequencies. Two of the pairs of field coils produce approximately homogeneous magnetic fields, which are necessary for reconstructing the orientation of the animal. The third pair produces a gradient field, which is necessary for reconstructing the position of the animal. Both sensor coils and leads are light enough (0.8–1.6 mg for three sensor coils of 40–80 windings, and 6.7 mg/m for the leads, causing a maximal load of approximately 5.7 mg) not to hinder normal flight of the animal (typical weight 80 mg). In general, the system can be used for high-speed recordings of head, eye or limb movements, where a wire connection is possible, but the mechanical load on the moving parts needs to be very small.

Keywords: Motion recording; Search coils; Three-dimensional eye movements; Insect flight; Optic flow; Blowfly

1. Introduction

In behavioural research it is often necessary to measure both the position and the orientation of moving animals, or of parts of their bodies, such as limbs or eyes. If the animal is fairly large and moves relatively slowly, video techniques are most convenient (Sandström et al., 1996). But if the animal is small and moves in a relatively large space, the typical spatial resolution of a video system may not be high enough to obtain a good estimate of the orientation. Moreover, the frame rate of conventional video systems may be too low for accurately monitoring details of the movement if the animal moves fast. We encountered such a situation when we embarked on a study of insect flight, with the purpose of reconstructing the dynamic visual stimulus and the optic flow (i.e. the field of local movements of the visual stimulus) as seen by the insect's visual system during flight. The blowflies used in this study (*Calliphora vicina*) move at a speed of up to 1 m/s in a restricted space (a cage of $0.4 \times 0.4 \times 0.4$ m^3, with a visual scene covering the walls), and make very fast turns of up to several thousand degree/s (for measurements in related species see Land and Collett, 1974; Collett and Land, 1975; Wagner, 1986; Land, 1993). The temporal and angular resolution of blowfly photoreceptors are in the order of 7 ms and 1.5°, respectively (full width at half maximum; Smakman et al., 1984; van Hateren, 1992). For an accurate reconstruction of the visual input, the temporal and angular resolution of the monitoring system recording how the

* Corresponding author. Fax: +31 50 3634740; e-mail: hateren@bcn.rug.nl

0165-0270/98/$19.00
PII S0165-0270(98)00069-7

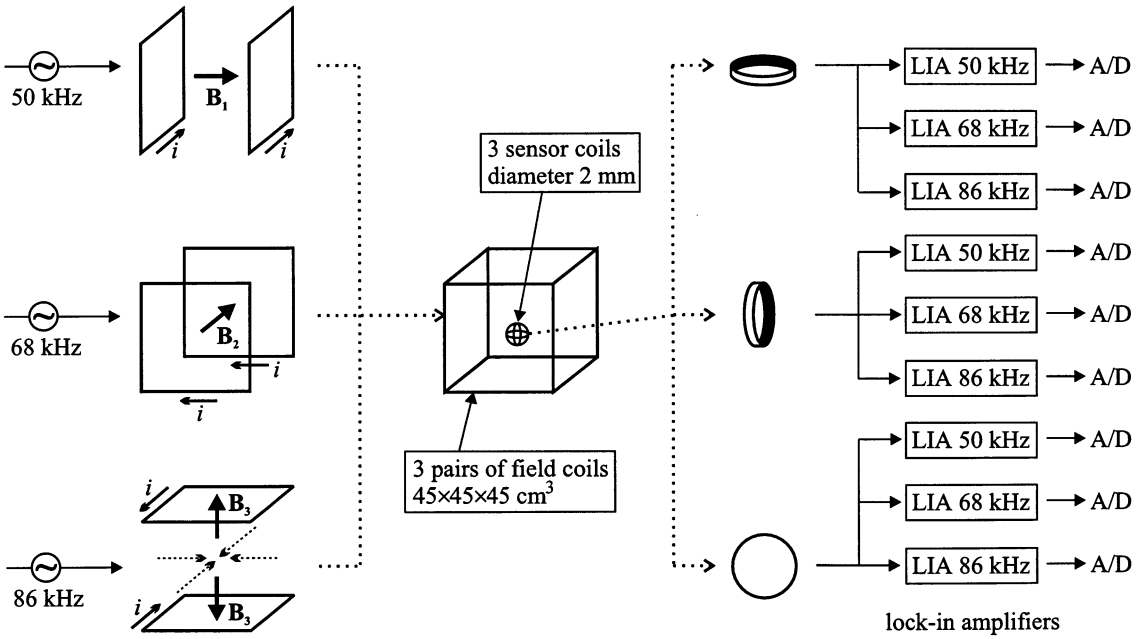

Fig. 1. Scheme of the set-up. Two pairs of field coils produce homogeneous magnetic fields $\vec{B}_1$ and $\vec{B}_2$ at 50 and 68 kHz, respectively, and a third pair of field coils produces a gradient field $\vec{B}_3$ at 86 kHz. These fields induce voltages in three orthogonal sensor coils, which are each connected to three lock-in amplifiers tuned to the field frequencies. The lock-in amplifiers give nine parameters, from which the orientation and position (six parameters) of the sensor coils can be reconstructed.

head moves during flight needs to be a few times better than these values. There is also a constraint on the spatial resolution, because it is related to the angular resolution: a positional error of 1 mm causes an error in orientation of up to 1° when a visual target is viewed from a distance of 6 cm (in a direction orthogonal to the direction of the positional error; in other directions the error is smaller). With this distance as a reasonable lower limit during flight, the resulting specifications for the monitoring system are a resolution of at least 2 ms in time, 0.5° in orientation (for each of three orientational angles), and 1 mm in position (for each of three spatial axes). This is beyond the capabilities of a conventional video system. Therefore, we decided to develop an alternative method that does meet the requirements. It is a variation on the well-known search coil technique for measuring eye and head movements (Ferman et al., 1987; Kasper et al., 1987; Schwenne and Zarnack, 1987, where it is applied to measuring wing movements in locust; Hess, 1990). In addition to giving the orientation of the sensor coils, as in earlier methods, our system also gives their position.

2. System description

2.1. Principle of operation

Fig. 1 shows a scheme of the set-up. Sinusoidal currents, with frequencies of 50, 68, and 86 kHz, flow through three orthogonal pairs of field coils. For two of these pairs, current flows in the same direction through each coil of the pair. As a result, the two magnetic fields are roughly homogeneous in the volume enclosed by the coils (Fig. 2A shows one of these fields). For the third pair, current flows in opposite directions through the two coils. As a result, the magnetic field is zero at the midpoint between the coils (Fig. 2B), and pointing in opposite directions close to the centers of the two coils. This gradient in the field occurs not only along the axis of symmetry connecting the centers of the coils (in Fig. 2B a vertical axis at the center of the figure), but also along any perpendicular axis through the midpoint between the coils (in Fig. 2B a horizontal axis at the center of the figure; see also Fig. 1, broken arrows in the lower left diagram). This means that each point in the volume has a unique magnetic field vector, i.e. with a unique combination of magnitude and direction. Therefore, an accurate measurement of the magnetic field vector produced by this third pair of coils will give the position within the measurement volume.

The time-varying magnetic field, produced by the superposition of the two homogeneous fields and the gradient field, induces voltages in three small orthogonal sensor coils (Fig. 3, inset). These sensor coils are each connected to three lock-in amplifiers, each tuned to one of the three frequencies present in the magnetic field. Thus a total of nine lock-in amplifiers yield nine parameters, from which the six parameters describing the orientation and position of the sensor coils can be

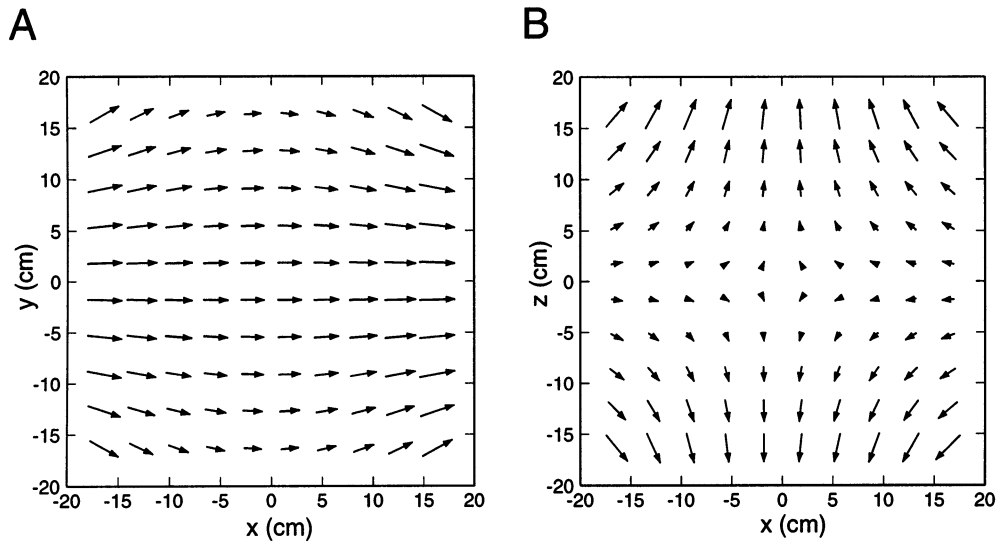

Fig. 2. (A) Magnetic field vectors as measured between a pair of coils, each oriented parallel to the y-z-plane (coils positioned at left and right borders in the figure; see also Fig. 1, upper left diagram), with currents running in the same direction through the coils. The resulting field is approximately homogeneous, and pointing in the x-direction, in a large part of the volume. (B) Magnetic field vectors as measured between a pair of coils, each oriented parallel to the x-y-plane (coils positioned at top and bottom borders in the figure; see also Fig. 1, lower left diagram), with currents running in opposite directions through the coils. The resulting field shows gradients in all directions (in the y-direction, not shown, similarly as in the x-direction).

extracted. This is possible, because the two homogeneous fields induce voltages in the sensor coils primarily related to their orientation, whereas the gradient field induces voltages in the sensor coils primarily related to their position. Two orthogonal sensor coils would suffice to determine orientation in the presence of two orthogonal homogeneous magnetic fields, but a third coil is necessary for determining the position using the gradient field. With three sensor coils, all three components of the gradient field vector can be measured, which then uniquely determines the position. The third sensor coil also enables measurement of orientation at positions in the volume where the homogenous fields deviate from homogeneity. The algorithm used for extracting the orientation and position from the measured parameters is described below in Section 2.4.

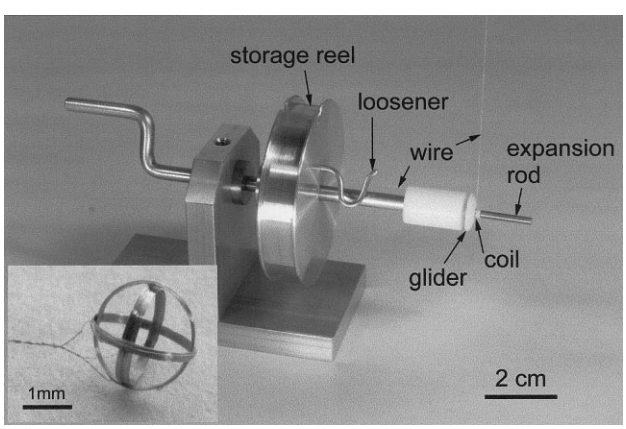

Fig. 3. Winder for producing small sensor coils. See text for further details. Inset: example of a system with three sensor coils.

2.2. Manufacturing the sensor coils

In order not to disturb the normal movement of those body parts under investigation, the weight of the sensor coils and of the connecting leads need to be much smaller than the weight of these body parts. Therefore, we use thin wire of 12-μm diameter (with two layers of insulation, 1 μm polyurethane and 1 μm polyvinylbutyral; Lotan-Fix, Huber and Suhner, Switzerland). The coils are produced by winding the wire around a hollow axis of flexible material (Teflon; see Fig. 3 for the device used for winding coils). Before winding, a thin metal expansion rod is inserted into the hollow axis; the fit is such that this slightly increases the diameter of the axis. Approximately 1 m of wire, later used for connecting the coil, is first wound on a storage reel. Subsequently, the coil is wound, and glued together by slightly heating the outer layer of the wire insulation. Removal of the metal rod loosens the coil from the axis, after which it can be shifted from the axis with the help of a tightly fitting glider (Fig. 3). To prevent breaking of the wire, a tension loosener loosens the wire before the coil is shifted from the axis. Finally, the wire is unwound from the storage reel, and twisted, by means of a motor, with the other wire originating from the coil. The tension during the twisting is controlled by hanging small weights at the end of each wire (Koch, 1980). Careful twisting is essential to prevent induction of voltage in the resulting leads.

With the technique described above, we are able to make coils as small as 0.8 mm in diameter, but for most experiments we used coils of 2-mm diameter, with 40 or 80 windings. This gives a good compromise between weight (0.8–1.6 mg for the three coils) and signal-to-noise ratio: the larger the diameter of the coils, and the more windings they have, the larger the signal that is induced and the better the signal-to-noise ratio. Coils of 2-mm diameter and 40 windings are light enough for mounting on either the head or the thorax of a blowfly (the typical weight of the head is only 8 mg, whereas the entire blowfly weighs typically 80 mg). Fig. 3 (inset) shows the resulting system of three coils. These were made with slightly different diameters (2.0, 2.1, and 2.2 mm) such that they fit within each other. The coils are fitted together as orthogonally as possible using a template with orthogonal grooves. In the calibration procedure (Section 2.4) their exact relative orientations are measured, and these actual orientations are used in the calculations performed for reconstructing the orientation and position of the blowfly.

2.3. Magnetic fields and lock-in amplifiers

The square field coils (with sides of 45 cm) are driven by power amplifiers (SMOS248, ILP Electronics, Canterbury, UK) with as source signal the output of the sine generators of three of the lock-in amplifiers. In order to increase the current through the coils (and thus the magnitude of the magnetic field and the voltage in the sensor coils), combinations of capacitors (polypropylene, total capacitance 7.2, 3.7, and 2.5 nF for frequencies 50, 68, and 86 kHz, respectively) are inserted in series with the coils, such that each circuit has a resonance frequency close to the driving frequency. As a result, the current through each of the field coils is approximately 3 A (peak-peak). With 25 windings, this results in a magnetic field of 0.15 mT (peak-peak) at the midpoint between the coils that produce a homogeneous field. The square windings of the field coils are made of 1.9-mm copper wire, at a distance (center-center) of 5 mm from each other in order to reduce the proximity effect (Terman, 1943). To reduce electrical coupling from the field coils to the sensor coils and their leads (Koch, 1980), the field coils are electrically shielded with a grounded fine mesh (which avoids significant eddy currents).

The sensor coils are connected to lock-in amplifiers (LIA-F-140, with a customized range of time-constants, Femto Messtechnik, Berlin, Germany). The lock-in amplifiers are in differential mode, which makes it possible to further reduce electrical coupling from the field coils to the leads by balancing the input impedances of the two inputs (by using a fixed resistor of 250 Ω in series with one lead of a sensor coil, and an adjustable resistor of 0–500 Ω in series with the other lead). The time-constant of the lock-in amplifiers was set at 1 ms (with the slope of the low-pass filter at 40 dB/dec), and their output was digitized by a 16-bit A/D-converter (Microstar DAP2416e, driven by Dasylab) at a sampling rate of 1 kHz, and stored on disk for off-line analysis.

2.4. Calibration and reconstruction

Although it is in principle possible to calculate the magnetic field from the configuration of the currents, the multiple windings in the field coils and the elaborate shielding makes this a complicated procedure. Therefore, we measured the magnetic fields directly. As the coils consist mainly of long straight wires carrying the current, it follows from the Biot-Savart law that the curvature of the magnetic field is in good approximation inversely related to the distance to the closest current. By keeping a (small) distance between the wall of the cage and the coils, there is a maximum to the curvature of the magnetic field within the measurement volume. This means that the magnetic field as a function of position is a band-limited signal. From the sampling theorem it then follows that the magnetic field at any point is completely determined by its values at a limited number of sampling points. For measuring the field at such a set of points, we constructed a set of three calibration coils, which were made orthogonal (within 0.3°) by winding them in grooves made on a cube of $1 \times 1 \times 1$ cm^3. When this set of coils is aligned with the coordinate system (defined by the orientation of the field coils), the output of each of these coils at a particular frequency is proportional to the amplitude of one component of the magnetic field vector at that frequency (i.e. due to a particular pair of field coils). Thus the nine lock-in amplifiers give directly the 3×3 vector components of the magnetic fields produced by the three pairs of field coils. Measurements were made with the calibration coils at $7 \times 7 \times 7$ positions evenly spaced throughout the measurement volume. Finally, for each magnetic field, the vector components were calculated on a $100 \times 100 \times 100$ lattice, where components at intermediate positions between the $7 \times 7 \times 7$ measured points were determined by cubic spline interpolation per component (using routines spline and splint from Press et al., 1992). The nine resulting sets of $100 \times 100 \times 100$ magnetic field components were stored, and used during the reconstruction to give, by linear interpolation, the magnetic field at any position.

The sensor coils (Fig. 3, inset) are made approximately orthogonal, but usually not exactly. In order to correct for any deviations from orthogonality, the system of three sensor coils was calibrated (see below). This calibration yields a 3×3 matrix that contains the exact orientation of each sensor coil, and its gain (which depends on the area and number of windings of

that coil). From the calibration of the magnetic field and the sensor coils, a forward model was constructed. This model predicts the output of the lock-in amplifiers as a function of the orientation and position of the sensor coils. This gives

$$\begin{bmatrix} L_{\alpha1}(\vec{r},\theta,\varphi,\psi) & L_{\alpha2}(\vec{r},\theta,\varphi,\psi) & L_{\alpha3}(\vec{r},\theta,\varphi,\psi) \\ L_{\beta1}(\vec{r},\theta,\varphi,\psi) & L_{\beta2}(\vec{r},\theta,\varphi,\psi) & L_{\beta3}(\vec{r},\theta,\varphi,\psi) \\ L_{\gamma1}(\vec{r},\theta,\varphi,\psi) & L_{\gamma2}(\vec{r},\theta,\varphi,\psi) & L_{\gamma3}(\vec{r},\theta,\varphi,\psi) \end{bmatrix} = \begin{bmatrix} C_{\alpha x} & C_{\alpha y} & C_{\alpha z} \\ C_{\beta x} & C_{\beta y} & C_{\beta z} \\ C_{\gamma x} & C_{\gamma y} & C_{\gamma z} \end{bmatrix}$$

$$\begin{bmatrix} \cos\theta\cos\varphi & \sin\theta\cos\varphi & -\sin\varphi \\ \cos\theta\sin\varphi\sin\psi-\sin\theta\cos\psi & \sin\theta\sin\varphi\sin\psi+\cos\theta\cos\psi & \cos\varphi\sin\psi \\ \cos\theta\sin\varphi\cos\psi+\sin\theta\sin\psi & \sin\theta\sin\varphi\cos\psi-\cos\theta\sin\psi & \cos\varphi\cos\psi \end{bmatrix} \begin{bmatrix} B_{1x}(\vec{r}) & B_{2x}(\vec{r}) & B_{3x}(\vec{r}) \\ B_{1y}(\vec{r}) & B_{2y}(\vec{r}) & B_{3y}(\vec{r}) \\ B_{1z}(\vec{r}) & B_{2z}(\vec{r}) & B_{3z}(\vec{r}) \end{bmatrix} \quad (1)$$

where $L_{\alpha1}(\vec{r},\theta,\varphi,\psi)$ is the output of the lock-in amplifier connected to the sensor coil α and tuned to the frequency of field coil pair 1, with the sensor coils at a position $\vec{r}$ and an orientation (θ,φ,ψ) in the measurement volume. The (row) elements $(C_{\alpha x},C_{\alpha y},C_{\alpha z})$ form the normal vector of sensor coil α when the three sensor coils are in their reference orientation, multiplied by the gain of sensor coil α. In practice, the (column) elements $(C_{\alpha x},C_{\beta x},C_{\gamma x})$ are measured directly as the outputs of the lock-in amplifiers tuned to field 1 and connected to sensor coils α, β, and γ when sensor coil α is approximately aligned with field 1 during the calibration of the sensor coils. Similarly, $(C_{\alpha y},C_{\beta y},C_{\gamma y})$ and $(C_{\alpha z},C_{\beta z},C_{\gamma z})$ are obtained for two other orthogonal orientations of the sensor coils with field 1 (approximately aligned with sensor coils β and γ, respectively). The middle matrix on the right side of Eq. (1) is a rotation matrix in the Fick gimbal system (Haslwanter, 1995), with θ the yaw (rotation around the vertical axis), φ the pitch (rotation around the horizontal axis perpendicular to the length axis of the animal), and ψ the roll (rotation around the length axis). Finally, $B_{1x}(\vec{r})$ is proportional to the x-component of the magnetic field due to field coils 1, at a position $\vec{r}$. In practice, this matrix element is measured during the field calibration as the output of the lock-in amplifier tuned to field 1 and connected to the calibration coil oriented in the x-direction, divided by the gain of this calibration coil (determined from the output obtained when it is mounted at the center of a homogeneous field, with the plane of the coil orthogonal to the field). In separate experiments we checked and verified the forward model of Eq. (1).

If we denote the set of nine outputs $L_{\alpha1}(\vec{r},\theta,\varphi,\psi),\ldots,L_{\gamma3}(\vec{r},\theta,\varphi,\psi)$ by a vector $\vec{L}(\vec{r},\boldsymbol{\theta,\varphi,\psi})$, the purpose of the reconstruction algorithm is to find those values of $\vec{r},\theta,\varphi$ and ψ (i.e. six parameters) that minimize the difference (in the least-squares sense) between the predicted $\vec{L}$ and the measured $\vec{L}$. This minimization is performed by a least-squares routine (amoeba, from Press et al., 1992), that gives

$$\min_{\vec{r},\theta,\varphi,\psi} \left\| \vec{L}_{\text{predicted}} - \vec{L}_{\text{measured}} \right\|^2 = \min_{\vec{r},\theta,\varphi,\psi} \left[\sum_{\substack{i=\alpha,\beta,\gamma \\ j=1,2,3}} \left(L_{ij,\text{predicted}}(\vec{r},\theta,\varphi,\psi) - L_{ij,\text{measured}}(\vec{r},\theta,\varphi,\psi)\right)^2 \right]. \quad (2)$$

This yields an estimate of the position $\vec{r}$ and orientation (θ,φ,ψ) at each time where a measurement was taken. This calculation takes about 4 ms per measured point on a fast work station (HP J280), which means that with a sampling rate of 1 kHz (1 ms per measurement) the reconstruction can be done within a reasonable time, only about four times longer than the experiment itself. It is probably possible to obtain better than real-time performance (thus enabling on-line reconstruction) by using a neural network trained to perform the reconstruction.

2.5. Accuracy

By moving the set of three sensor coils repeatedly along a known trajectory at various positions within the measurement volume, we estimated the systematic and random (stochastic) errors of the system (see Fig. 4A for an example). Systematic errors are important if an absolute reconstruction of the viewing direction and position is required. Random errors are important for relative variations of viewing direction, e.g. as needed for the angular speed of gaze shifts. Due to the shape of the fields (Fig. 2), the errors in the position and orientation depend on the distance from the center of the measurement volume. We found systematic errors (primarily due to small errors in the field calibration) for the orientational angles of 0.2 and 0.3° (for sensor coils with 80 and 40 windings, respectively) in the central half of the measurement volume (i.e. a central cube with 30-cm sides), gradually rising to 0.7 and 1° (80 and 40 windings) in the corners of the measurement volume. Random errors (standard deviations) in orientational angles were 0.15 and 0.3° (80 and 40 windings) in the central volume, up to 0.3 and 0.5° in the corners. Systematic errors in the position were 1.5 and 2 mm (80 and 40 windings) in the central volume, up to 3 and 5 mm (80 and 40 windings) in the corners; random errors in the position were 0.5 and 0.7 mm (80 and 40 windings) in the central volume, up to 0.7 and 1 mm (80 and 40 windings) in the corners.

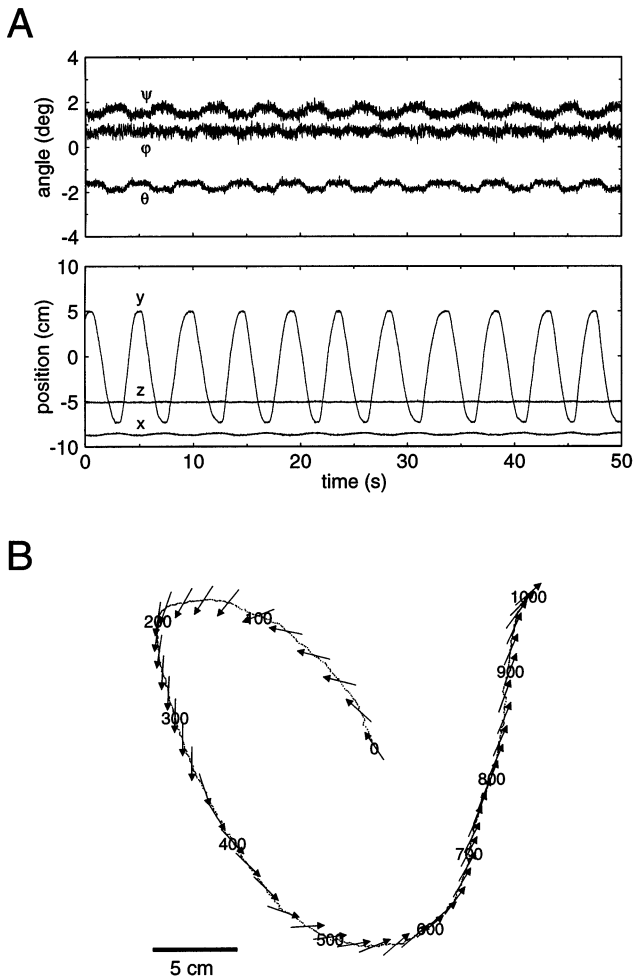

Fig. 4. (A) Traces recorded whilst moving the sensor coils, by hand, along a guiding rail in the y-direction. The small, systematic variations in the other coordinates (x, z, θ, φ and ψ) are absolute errors due to small deviations in the field calibration. The noise in the traces (arising from noise in the electronics) gives an impression of the precision (i.e. random errors) of the system. (B). Example of a flight path, recorded from the thorax of a flying blowfly. The three-dimensional path (in this case almost confined to a horizontal plane) was projected on a horizontal plane. Dots show positions at consecutive ms (starting at ms 0, ending at ms 1000), the arrows the orientation of the thorax at 20-ms intervals.

The random errors can be reduced by using magnetic fields that are stronger or have a higher frequency, by increasing the diameter or the number of windings of the sensor coils, or by improving the signal-to-noise ratio of the electronics. In our system, the total resistance of sensor coils, leads and balancing resistances is approximately 1 kΩ, and the lock-in amplifiers are measuring voltage. If this resistance is reduced (e.g. with shorter leads, or wire of larger diameter), the signal-to-noise ratio will become better by using lock-in amplifiers that measure current, or by using a specialized system like that designed and manufactured by Remmel (1984).

The systematic errors arise mainly from small errors in the calibration of the magnetic field, mostly due to the interpolation. These errors can be reduced by increasing the number of points where the field is measured. Another potential improvement is the use of a better interpolation procedure than cubic spline interpolation. As the magnetic fields are relatively slowly varying in time, the differential equation to which they obey is fairly simple (the Laplace equation for the magnetic scalar potential; Jackson, 1975). It may thus be quite feasible to use this extra information about the shape of the magnetic fields to improve the estimate of the magnetic field, both at and between the measured points.

3. Application

A set of three sensor coils of 2-mm diameter each, consisting of 80 windings, was attached to the thorax of a blowfly. The leads were led to the abdomen, and, via a free stretch of approximately 80 cm, to the bottom of the cage, and finally to the lock-in amplifiers. Total weight of coils and leads (approximately 7 mg) was much smaller than the weight of a blowfly (typically 80 mg). The coils and leads did not appear to hinder normal free flight, which was checked by comparing flight performance with different weights of the coils and leads. The walls of the cage were covered with transparencies onto which a natural image (primarily foliage) was printed. The walls were illuminated from the outside through frosted paper.

Fig. 4B shows an example of a horizontal projection of a reconstructed flight path. The total duration of the stretch shown is 1 s, with the dots denoting the position at 1-ms intervals. The arrows show the orientation of the thorax, shown only at 20-ms intervals for the sake of clarity. As can be seen in the figure, turns by the thorax can be very fast (e.g. a turn of more than 60° in 40 ms at time 100 ms), and the orientation of the thorax is more involved in the dynamics of turning than in aligning with the direction of forward motion.

4. Conclusion

The system described here solves the problem we were faced with: measuring, with sufficient accuracy, the orientation and position of a small, fast-moving animal. By reducing the time constants of the lock-in amplifiers, the system can be adjusted for even faster movements (although this would increase the noise in the output, and thus reduce the orientational and spatial resolution). Alternatively, if it is possible to use heavier sensor coils, the accuracy of the system can be improved appreciably by increasing the diameter or number of windings of the sensor coils. This flexibility makes the system well suited for a range of applications in behavioural research.

Acknowledgements

We thank Marten Jansen, Herman Snippe, and Esther Wiersinga-Post for comments. This research was supported by the Netherlands Organization for Scientific Research (NWO).

References

Collett TS, Land MF. Visual control of flight behaviour in the hoverfly, *Syritta pipiens* L. J Comp Physiol 1975;99:1–66.

Ferman L, Collewijn H, Jansen TC, van den Berg AV. Human gaze stability in the horizontal, vertical and torsional direction during voluntary head movements, evaluated with a three-dimensional scleral induction coil technique. Vis Res 1987;27:811–28.

Haslwanter T. Mathematics of three-dimensional eye rotations. Vis Res 1995;35:1727–39.

van Hateren JH. Theoretical predictions of spatiotemporal receptive fields of fly LMCs, and experimental validation. J Comp Physiol A 1992;171:157–70.

Hess BJM. Dual-search coil for measuring 3-dimensional eye movements in experimental animals. Vis Res 1990;30:597–602.

Jackson JD. Classical Electrodynamics. New York: Wiley, 1975.

Kasper HJ, Hess BJM, Dieringer N. A precise and inexpensive magnetic field search coil system for measuring eye and head movements in small laboratory animals. J Neurosci Methods 1987;19:115–24.

Koch UT. Analysis of cricket stridulation using miniature angle detectors. J Comp Physiol 1980;136:247–56.

Land MF. Chasing and pursuit in the dolichopodid fly *Poecilobothrus nobilitatus*. J Comp Physiol A 1993;173:605–13.

Land MF, Collett TS. Chasing behaviour of houseflies (*Fannia canicularis*). J Comp Physiol 1974;89:331–57.

Press WH, Teukolsky SA, Vetterling WT, Flannery BP. Numerical Recipes in Fortran. New York: Cambridge University Press, 1992.

Remmel RS. An inexpensive eye movement monitor using the scleral search coil technique. IEEE Trans Biomed Eng 1984;31:388–90.

Sandström G, Bäckström A, Olsson KÅ. REMAC: a video-based motion analyser interfacing to an existing flexible sampling system. J Neurosci Methods 1996;69:205–11.

Schwenne T, Zarnack W. Movements of the hindwings of *Locusta migratoria*, measured with miniature coils. J Comp Physiol A 1987;160:657–66.

Smakman JGJ, van Hateren JH, Stavenga DG. Angular sensitivity of blowfly photoreceptors: intracellular measurements and wave-optical predictions. J Comp Physiol A 1984;155:239–47.

Terman FE. Radio Engineers' Handbook. New York: McGraw-Hill, 1943.

Wagner H. Flight performance and visual control of flight of the free-flying housefly (*Musca domestica* L.). I. Organization of the flight motor. Phil Trans R Soc Lond B 1986;312:527–51.